Int. J. Heat Mass Transfer. Vol. 26, No. 12, pp. 1805-1814, 1983
Printed in Great Britain

0017-9310/83 $3.00+0.00

NATURAL CONVECTION IN VERTICALLY AND HORIZONTALLY LAYERED POROUS MEDIA HEATED FROM THE SIDE

D. POULIKAKOS* and A. BEJAN
Department of Mechanical Engineering, Campus Box 427, University of Colorado, Boulder, CO 80309, U.S.A.

(*Received* 24 *January* 1983 *and in final form* 17 *March* 1983)

Abstract—The effect of nonuniform permeability and thermal diffusivity on natural convection through a porous system heated from the side is investigated numerically. The first part of the study, in Section 2, focuses on systems composed of vertical sublayers. It is shown that the heat transfer rate is influenced substantially by the thickness and permeability of the peripheral sublayers adjacent to the heated vertical walls. The heat transfer results are correlated by using the ratio of peripheral sublayer thickness divided by the boundary layer thickness based on peripheral sublayer properties. The second part of the study, in Section 3, deals with porous systems composed of horizontal sublayers with different permeabilities. It is shown that due to the lack of homogeneity the vertical walls of the system are lined by boundary layers whose thicknesses vary from one sublayer to the next. A general heat transfer scaling law for horizontally layered systems is reported.

NOMENCLATURE

c_p	fluid specific heat at constant pressure
d	sublayer thickness
g	gravitational acceleration
G	dimensionless group for horizontally-layered systems, equation (26)
H	vertical dimension
k	thermal conductivity of fluid/porous matrix composite
K	permeability
L	horizontal dimension
Nu	Nusselt number, equations (16) and (25)
P	pressure
Q	net heat transfer rate, equation (17) [$\mathrm{Wm^{-1}}$]
Ra	Rayleigh number based on H, equation (14)
T	temperature
T_C	right wall temperature (cold)
T_H	left wall temperature (hot)
ΔT	temperature difference, $T_H - T_C$
u	horizontal velocity component
v	vertical velocity component
x	horizontal Cartesian coordinate
y	vertical Cartesian coordinate.

Greek symbols

α	thermal diffusivity of porous medium, $k/\rho c_p$
β	coefficient of thermal expansion
δ_T	thermal boundary layer thickness
μ	viscosity
ν	kinematic viscosity, μ/ρ
ρ	fluid density
ψ	streamfunction.

Subscripts

i	pertaining to the ith sublayer, $i = 1,\ldots,n$
f	pertaining to the fluid.

Other symbols

$\hat{}$	dimensionless quantity.

* Present address: Department of Mechanical Engineering, University of Illinois at Chicago, P.O. Box 4348, Chicago, IL 60680, U.S.A.

1. INTRODUCTION

THE HEAT transfer induced by buoyancy effects in fluid-saturated porous media has attracted considerable attention during the past decade. The interest in this fundamental topic is fueled by applications in many real-life situations ranging from thermal insulation engineering to geothermal energy extraction. A large cross section of the fundamental research contributed to this topic has been reviewed in a recent paper [1].

In the context of thermal insulation applications, which is the focus of Section 2 and the main part of the present study, one can identify a large class of convection problems consisting of a two-dimensional porous system confined between two differentially-heated vertical walls and two adiabatic horizontal walls. The research devoted to this class of problems is relatively new. A number of early experiments demonstrated that the net heat transfer rate across the porous layer increases monotonically as the Rayleigh number increases [2–4]. These measurements were verified later by Bankvall [5] in a numerical study which simulated the steady-state convection pattern in the range $0.5 < H/L < 50$ and $1 < Ra < 200$. Similar results were obtained by Chan *et al.* [6] and Burns *et al.* [7].

The theoretical work on natural convection heat transfer through a porous layer heated and cooled from the side was pioneered by Weber [8] who developed an Oseen-linearized solution for the boundary layer regime in a very tall layer ($H/L \gg 1$). The Weber solution was modified later by Bejan [9] to account for the net heat transfer which takes place vertically through the core region of moderately tall layers. Simpkins and Blythe [10] reported an alternative theory for the boundary layer regime based on an original closed-form solution [11]. Simpkins and Blythe [10] showed that the boundary layer theories of refs. [8–10] account satisfactorily for the net heat transfer rates reported experimentally and numerically for high Rayleigh numbers in tall layers in the steady state.

A number of studies have shown that the thermal convection pattern in a shallow ($H/L < 1$) configuration can differ greatly from the pattern described experimentally [4], numerically [5–7] and theoretically [8–10] in tall spaces. Walker and Homsy [12] developed an asymptotic solution for the flow and temperature fields inside a shallow layer using the aspect ratio as the small parameter. They showed that unlike in tall layers the core region plays an active role in the heat transfer process. An approximate integral-type solution for the same geometry was proposed by Bejan and Tien [13]. Most recently, the shallow geometry was the subject of a numerical study [14]. The patterns of isotherms and streamlines published in ref. [14] differ substantially from the patterns in tall layers [5, 6], suggesting that the mechanics of shallow layer circulation differs fundamentally from that of tall layers.

The literature survey presented above demonstrates that our knowledge of natural convection in porous layers heated from the side is constrained by the idea (the model) that the porous layer is *homogeneous*. In real life, however, most porous insulation systems are inhomogeneous, partly due to fabrication procedures and partly (more often) due to installation by human hand. The inhomogeneity of the porous medium makes it possible for certain regions of the medium to play the decisive role with regard to the thermal insulation capability of the system. If, for example, the porous material is packed so that the permeability of near-wall regions is greater than the permeability of far regions, then the buoyancy-driven flow will be *channeled* along the walls.

The importance of flow channeling and porous medium inhomogeneity was recognized at the most recent Natural Convection Workshop [15]. Thus, the main objective of the present study is to determine the effect of porous medium inhomogeneity on heat transfer through a vertical layer heated from the side. In particular, we seek to establish the heat transfer effect of 'flow channeling'; that is, the effect of relatively more permeable regions situated adjacent to the vertical walls.

In Section 3 we document the effect of porous matrix inhomogeneity on heat transfer through a horizontal layer. Motivated by geophysical applications, we consider a horizontal layer model consisting of two individually homogeneous sublayers. This model simulates the flow driven through high-permeability layers by temperature gradients existing in the horizontal direction. The opposite situation, i.e. the inhomogeneous porous medium flow driven by temperature gradients in the direction of the earth's radius, was investigated in a recent paper [16].

2. VERTICAL LAYERS

2.1. *Mathematical formulation*

Consider a two-dimensional rectangular cavity filled with a fluid saturated multilayered porous medium. The overall dimensions of the layer are H and L, Fig. 1. It is assumed that this porous layer is made up of n separately homogeneous and isotropic vertical sublayers.

In accordance with the homogeneous porous medium model [1], the equations governing the conservations of mass, momentum and energy in the ith layer in the steady state are:

$$\frac{\partial u}{\partial x}+\frac{\partial v}{\partial y}=0, \tag{1}$$

$$u=-\frac{K_i}{\mu}\frac{\partial P}{\partial x}, \tag{2}$$

$$v=-\frac{K_i}{\mu}\left(\frac{\partial P}{\partial y}+\rho g\right), \tag{3}$$

$$u\frac{\partial T}{\partial x}+v\frac{\partial T}{\partial y}=\alpha_i\left(\frac{\partial^2 T}{\partial x^2}+\frac{\partial^2 T}{\partial y^2}\right), \tag{4}$$

where u, v, μ, P and T are the fluid velocity components, the viscosity, the pressure and the temperature, respectively. The two momentum equations are based on the Darcy flow model and K_i represents the permeability of the porous matrix of the ith layer. The effective thermal diffusivity is defined as $\alpha_i = k_i/(\rho c_p)_f$ where k_i is the thermal conductivity of the ith porous sublayer filled with stagnant fluid. It is assumed that the fluid is locally in thermal equilibrium with the solid porous structure.

Invoking the Boussinesq approximation,

$$\rho=\rho_0[1-\beta(T-T_0)],$$

eliminating the pressure terms between equations (2) and (3), and introducing the streamfunction

$$u=\frac{\partial\psi}{\partial y},\quad v=-\frac{\partial\psi}{\partial x} \tag{5}$$

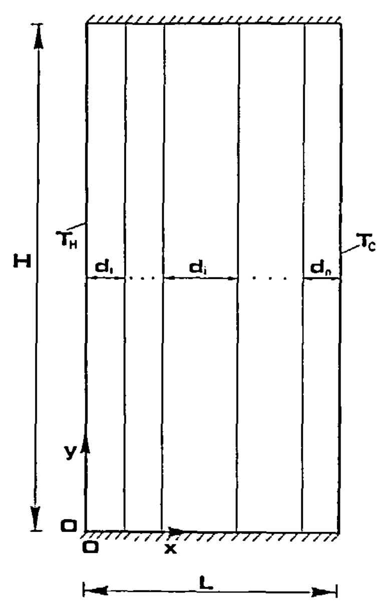

FIG. 1. Schematic of a rectangular space filled with a fluid-saturated multilayered porous material.

yields a unique momentum conservation statement

$$\left(\frac{\partial^2}{\partial x^2}+\frac{\partial^2}{\partial y^2}\right)\psi = -\frac{K_i g\beta}{\nu}\frac{\partial T}{\partial x}. \quad (6)$$

The multilayered porous matrix/fluid system is surrounded by solid boundaries described by

$$u = 0, \quad T = T_H \quad \text{at } x = 0, \quad (7)$$

$$u = 0, \quad T = T_C \quad \text{at } x = L, \quad (8)$$

$$v = 0, \quad \frac{\partial T}{\partial y} = 0 \quad \text{at } y = 0, H. \quad (9)$$

The above boundary conditions account for the impermeability of the rectangular cavity and the fact that the two horizontal walls are adiabatic, while the two vertical walls are kept at different temperatures, T_H and T_C, with $T_H > T_C$.

In what follows, we determine numerically the effect of sublayering, specifically the effect of 'channeling', i.e. the case of maximum permeability near the vertical walls, and the effect of 'packing', or the case of least permeability near the walls. We document these effects by focusing on a three-sublayer model of the porous system of Fig. 1.

2.2. *Numerical solution*

Selecting H, α_1, and $\Delta T = T_H - T_C$ as reference units for length, streamfunction and temperature variation, respectively, we define the following dimensionless variables

$$\hat{x} = x/H, \quad \hat{y} = y/H, \quad \hat{\psi} = \psi/\alpha_1, \quad \hat{T} = \frac{T-T_C}{T_H-T_C}. \quad (10)$$

The corresponding form of the governing equations and boundary conditions is

$$\left(\frac{\partial^2}{\partial \hat{x}^2}+\frac{\partial^2}{\partial \hat{y}^2}\right)\hat{\psi} = -Ra_1\frac{\alpha_1}{\alpha_i}\frac{K_i}{K_1}\frac{\partial \hat{T}}{\partial \hat{x}}, \quad (11)$$

$$\frac{\partial}{\partial \hat{x}}(\hat{u}\hat{T})+\frac{\partial}{\partial \hat{y}}(\hat{v}\hat{T}) = \frac{\alpha_i}{\alpha_1}\left(\frac{\partial^2}{\partial \hat{x}^2}+\frac{\partial^2}{\partial \hat{y}^2}\right)\hat{T}, \quad (12)$$

$$\hat{u} = 0, \quad \hat{\psi} = 0 \quad \text{and} \quad \hat{T} = 1 \quad \text{at} \quad \hat{x} = 0,$$

$$\hat{u} = 0, \quad \hat{\psi} = 0 \quad \text{and} \quad \hat{T} = 0 \quad \text{at} \quad \hat{x} = L/H, \quad (13)$$

$$\hat{v} = 0, \quad \hat{\psi} = 0 \quad \text{and} \quad \frac{\partial \hat{T}}{\partial \hat{y}} = 0 \quad \text{at} \quad \hat{y} = 0$$

$$\hat{v} = 0, \quad \hat{\psi} = 0 \quad \text{and} \quad \frac{\partial \hat{T}}{\partial \hat{y}} = 0 \quad \text{at} \quad \hat{y} = 1,$$

where Ra_1 is the Darcy-modified Rayleigh number based on the height of the enclosure and the properties of the porous sublayer adjacent to the warm (left) wall

$$Ra_1 = \frac{K_1 g\beta H(T_H - T_C)}{\nu\alpha_1}. \quad (14)$$

The dimensionless formulation (11)–(13) shows the emergence of two more dimensionless groups (in addition to the usual, Ra_1 and H/L), namely, the relative permeability K_i/K_1 and the relative thermal diffusivity α_i/α_1.

The numerical solution of equation (12) was determined using the unconditionally stable finite difference scheme proposed by Allen and Southwell [17], which was improved and tested successfully by Chow and Tien [18]. The Allen–Southwell method is an exponential scheme: its detailed formulation is omitted here, for it can be found in refs. [17, 18]. The streamfunction field was obtained from equation (11) using the successive over-relaxation method [19] and a known temperature distribution.

The region of interest was covered with m vertical and l horizontal grid lines; the grid fineness $m \times l = 41 \times 81$ was used for the present solution, even though $m \times l = 21 \times 41$ yielded very reasonable results. The final flow and temperature fields resulted from an iterative process that was repeated until the following criterion was satisfied

$$\frac{\sum_{i=1}^{m}\sum_{j=1}^{l}|\phi_{i,j}^{r+1}-\phi_{i,j}^{r}|}{\sum_{i=1}^{m}\sum_{j=1}^{l}|\phi_{i,j}^{r+1}|} < 10^{-5}. \quad (15)$$

In criterion (15) ϕ refers to $\hat{T}$ and $\hat{\psi}$, and r denotes the iterative cycle.

The effect of fluid motion on the heat transfer between the two vertical walls of the porous layer was evaluated by computing the conduction-referenced Nusselt number

$$Nu = \frac{Q}{H(T_H - T_C)/\sum_{i=1}^{n}(d_i/k_i)}, \quad (16)$$

where d_i and k_i are the thickness and the overall fluid/porous matrix conductivity of the ith sublayer of the system (see Fig. 1). The overall heat transfer rate Q is defined as

$$Q = -\int_0^H k_1\left(\frac{\partial T}{\partial x}\right)_{x=0} dy. \quad (17)$$

In terms of dimensionless quantities, equation (10), the Nusselt number reads

$$Nu = -\left(\sum_{i=1}^{n}\frac{d_i}{H}\frac{k_1}{k_i}\right)\int_0^1\left(\frac{\partial \hat{T}}{\partial \hat{x}}\right)_{\hat{x}=0} d\hat{y}. \quad (18)$$

Equation (18) was integrated numerically after the final temperature field was obtained. A relation similar to equation (18) is obtained by integrating the heat flux along the cold wall located at $x = L$. This second Nusselt number calculation was carried out, and the results were found to be nearly identical to the values yielded by equation (18); the discrepancy between the results to the two approaches was less than 1.5% throughout this study.

2.3. *Flow and temperature fields*

Since in many fibrous insulation systems, the conductivity of the fluid (air) dominates the aggregate conductivity of the fluid-saturated porous composite [16], the calculations reported in this paper are based on the assumption that the thermal diffusivity of the

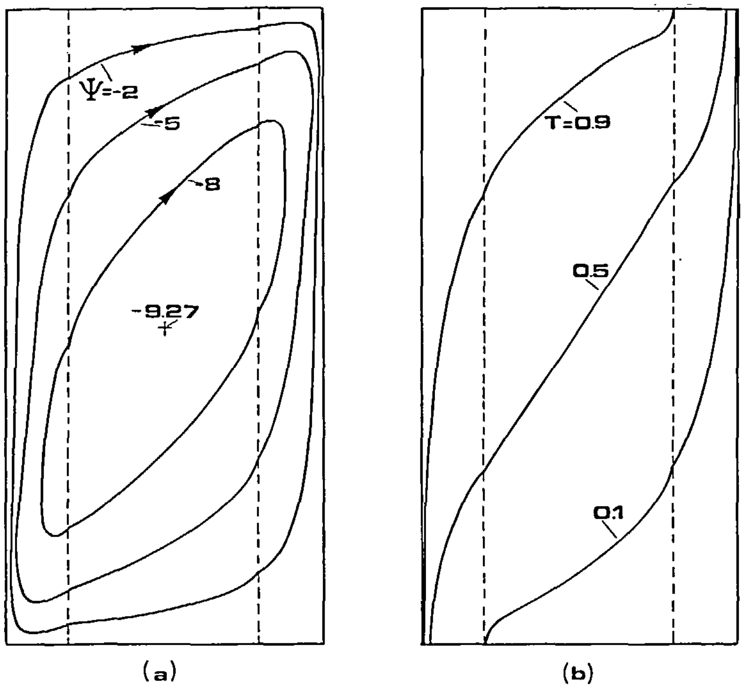

FIG. 2. Numerical solution for $H/L = 2$, $Ra_1 = 500$, $n = 3$, $d_1/L = d_3/L = 0.2$, $K_2/K_1 = 0.2$, $K_3/K_1 = 1$, $\alpha_1 = \alpha_2 = \alpha_3$. (a) Streamline pattern, (b) isotherm pattern.

porous medium (α) is independent of position. This assumption served to isolate the effect of channeling or packing, i.e. the effect of the permeability function K_i/K_1 on the net heat transfer rate through the porous system.

The effect of flow channeling along the vertical walls of a porous layer is shown by the three-sublayer model in Fig. 2. The permeability of the two outer sublayers is five times greater than the permeability of the core region. At a relatively high Rayleigh number, $Ra_1 = 500$, the vertical flow takes place primarily through the more permeable vertical sublayers, hence, the naming of this effect as 'channeling'. The two outer sublayers exchange fluid mainly through the upper and lower ends of the inner, less permeable, region. It is worth noting that the step variation in permeability across the interfaces of the different sublayers induces step changes in the slopes of both streamlines and isotherms. The abrupt change in the slope of the $T =$ constant line is required by the conservation of energy across the interfaces, keeping in mind that this energy flow is due to a combination of thermal diffusion and enthalpy flow.

The opposite effect, the effect of packing associated with relatively less permeable outer sublayers, is shown in Fig. 3. The more permeable inner region appears to 'attract' the flow: this property renders the isotherms of this region almost horizontal and yields a vertically stratified core.

2.4. *Heat transfer results*

The ultimate objective of the present study was to establish the effect of nonuniform permeability on heat transfer. We pursued this objective on two fronts: on the one hand by calculating the heat transfer rate numerically and documenting it as in Figs. 4(a) and (b) and, on the other hand, by relying on scaling analysis to explain the observed trends and to correlate the numerical heat transfer results, as in Figs. 5(a) and (b).

The effect of channeling on heat transfer is shown in Fig. 4(a). The conduction-referenced Nusselt number increases steadily as the channel thickness d_1/L increases and, as one would expect, as the Rayleigh number increases. The chief message of Fig. 4(a) is that in the high-Rayleigh-number regime the net heat transfer rate is influenced strongly by the thickness of the wall sublayers of maximum permeability. The reverse trend is observed if the permeability of the wall sublayers is less than the permeability of the core sublayer. As shown in Fig. 4(b), the heat transfer rate decreases as the wall sublayer thickness d_1/L increases; the effect becomes more and more pronounced as the Rayleigh number increases; in other words, as the convection phenomenon is dominated by vertical boundary layers.

To explain the above heat transfer trends, we recall first that in the boundary layer regime the Nusselt number scales mainly as [8]

$$Nu \sim Ra^{1/2}, \tag{19}$$

where Ra is the Rayleigh number based on height H and wall-to-wall temperature difference. Furthermore, in a homogeneous porous layer the thickness of each vertical boundary layer scales as [8]

$$\delta_T \sim H\ Ra^{-1/2}. \tag{20}$$

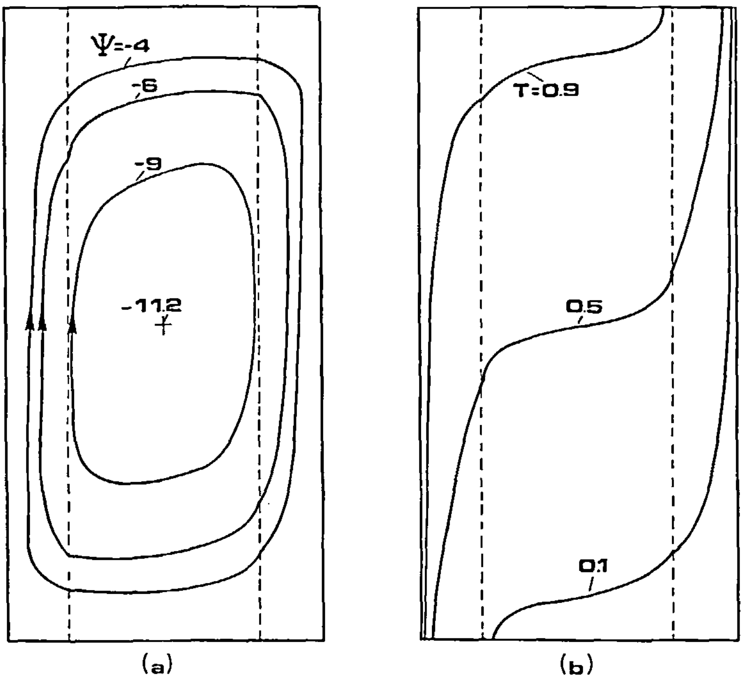

FIG. 3. Numerical solution for $H/L = 2$, $Ra_1 = 200$, $n = 3$, $d_1/L = d_3/L = 0.2$, $K_2/K_1 = 5$, $K_3/K_1 = 1$, $\alpha_1 = \alpha_2 = \alpha_3$. (a) Streamline pattern, (b) isotherm pattern.

Turning our attention to the case of heat transfer through a layer with high-permeability sublayers near the vertical walls (channeling), it is reasonable to expect that the Nu variation shown in Fig. 4(a) is due to the competition between two length scales, the boundary layer thickness δ_T and the sublayer thickness d_1. Indeed, by plotting the $Nu - d_1/L$ data of Fig. 4(a) as $Nu/Ra_1^{1/2}$ vs d_1/δ_T, it is possible to correlate the heat transfer calculations so that the results fall on what appears to be a single curve [see Fig. 5(a)].

The important conclusion to be drawn from Fig. 5(a) is that the high-permeability sublayers influence the overall heat transfer rate if their thickness is of the same order of magnitude or greater than the thermal boundary layer thickness. This conclusion is reinforced by Fig. 5(b), which shows the $Nu/Ra_2^{1/2} - d_1/\delta_T$ correlation of the heat transfer data of Fig. 4(a) for a layer with a high-permeability core. Note that in this case Nu scales as $Ra_2^{1/2}$, where Ra_2 is based on the high permeability located in the core. In the case of channeling, Fig. 5(a), Nu scales as $Ra_1^{1/2}$, where again Ra_1 is based on the high permeability of the peripheral sublayers.

3. HORIZONTAL LAYERS

The effect of porous matrix inhomogeneity on natural convection through horizontal layers can be

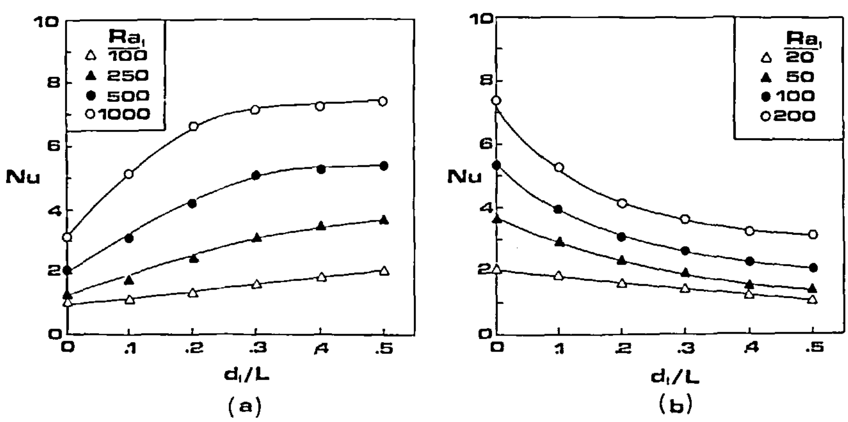

FIG. 4. The relationship between the heat transfer rate and the thickness of the peripheral sublayer ($n = 3$, $d_1 = d_3$, $K_1 = K_3$, $\alpha_1 = \alpha_2 = \alpha_3$). (a) The peripheral layers have the highest permeability, $K_2/K_1 = 0.2$. (b) The core layer has the highest permeability, $K_2/K_1 = 5$.

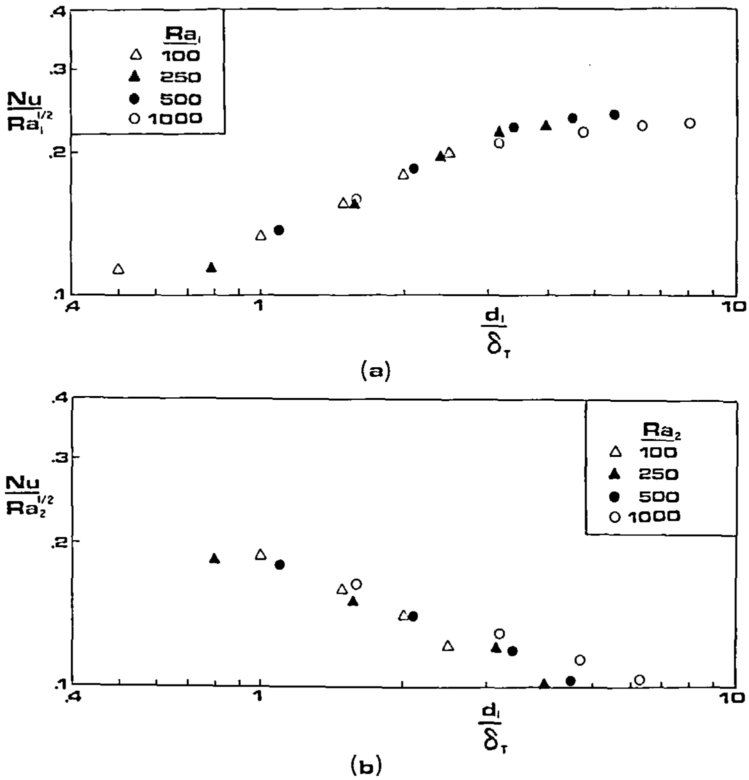

FIG. 5. Correlation of the heat transfer data of Figs. 6(a) and (b). (a) $K_2/K_1 = 0.2$, (b) $K_2/K_1 = 5$.

analyzed in the same manner as the vertical layers of Section 2. However, due to space limitations, this section will only focus briefly on the case of convection in a two-sublayer horizontal system (Fig. 6). From the outset, we expect to encounter a (heat transfer)–(permeability) relationship different than in Section 2, as the heat transfer mechanism in horizontal layers differs markedly from that in tall vertical layers [13, 14].

Consider the system of Fig. 6 where $H/L = 0.5$ and the upper sublayer is five times more permeable than the lower, $K_2/K_1 = 5$. Assuming once again that the thermal conductivity of the fluid dominates the aggregate conductivity of the porous composite [16], we take α as uniform throughout the system: in this way, we isolate the role played by the permeability function K_2/K_1 on the end-to-end heat transfer through the system. The mathematical and numerical formulation employed previously (Sections 2.1 and 2.2) applies to this convection problem as well; however, in this case the grid fineness used is $m \times l = 81 \times 41$. A representative set of isotherms and streamlines is presented in Figs. 6(a) and (b) for $Ra_1 = 150$, where Ra_1 is based on the end-to-end ΔT, the overall height of the system, H, and the low permeability K_1. The streamlines show that the cellular flow prefers the more permeable upper half of the system. The streamline pattern is no longer centrosymmetric (as in homogeneous systems [14]); instead, the streamfunction maximum is located in the upper half, near the 'starting corner' of the cold vertical boundary layer.

The map of isotherms, Fig. 6(b), reveals the existence of strong convective effects in the establishment of the temperature field. Distinct thermal layers are aligned with the vertical walls of the porous medium. The vertical boundary layers are sharper in the more permeable half of the system, as expected.

Figures 7(a) and (b) show the effect of permeability and inhomogeneity on heat transfer. In particular, Fig. 7(a) shows that the conduction-referenced Nusselt number Nu increases rather sharply as K_2/K_1 increases, i.e. as the channel provided by the upper sublayer becomes more permeable. Increasing the Rayleigh number Ra_1 has the effect of increasing both the Nusselt number and the slope of each $Nu\,(K_2/K_1)$ curve.

Finally, Fig. 7(b) shows the effect of varying the sublayer height ratio d_1/H, where d_1 is the height of the lower (less permeable) sublayer. Note that for $d_1/H < 0.1$ and $d_1/H > 0.9$ the effect of d_1/H on Nu becomes less dramatic: in the former case, the less permeable layer is too small to seriously influence the net heat transfer, while in the latter most of the fluid has already been discharged from the vertical boundary layers into the core, and a further increase in d_1/H is not likely to enhance by much the convective heat transfer contribution to the net heat transfer through the system.

The heat transfer trends exhibited in Figs. 7(a) and (b) can be predicted and correlated based on scale analysis. The streamline pattern of Fig. 6(a) shows that the thickness of each vertical boundary layer decreases sharply across the interface separating the two

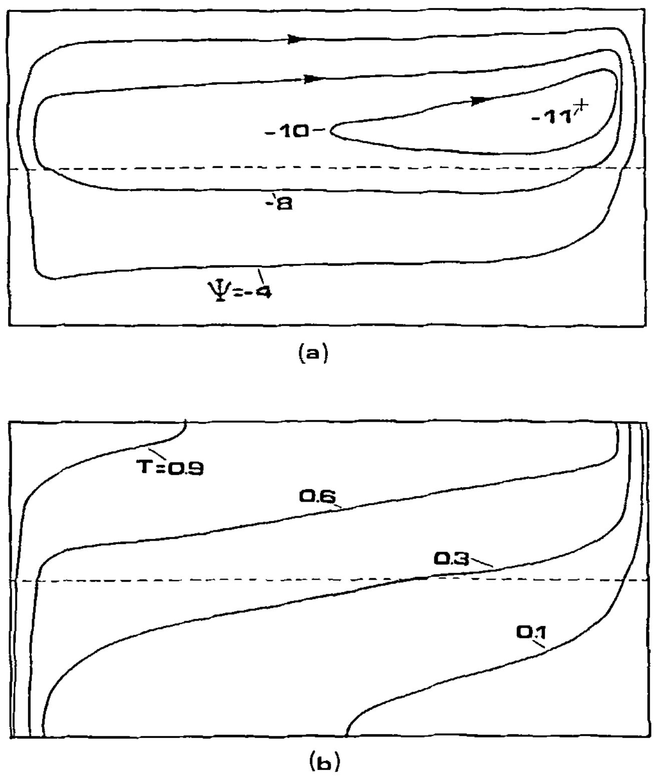

FIG. 6. Numerical solution for $H/L = 0.5$, $Ra_1 = 150$, $n = 2$, $d_1 = d_2$, $K_2/K_1 = 5$, $\alpha_2/\alpha_1 = 1$. (a) Streamline pattern, (b) isotherm pattern.

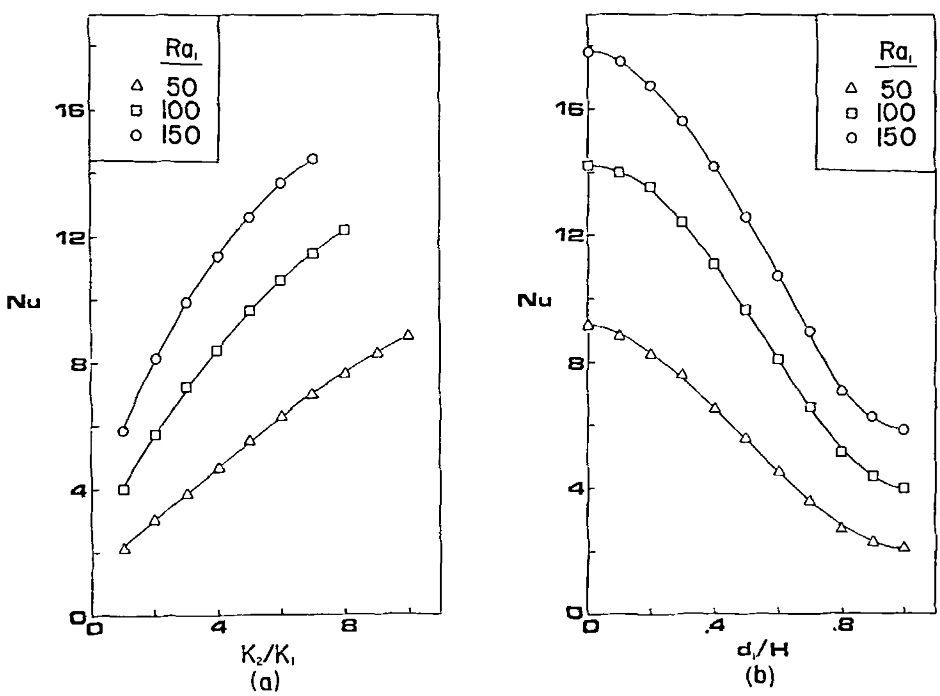

FIG. 7. Heat transfer through a horizontally layered system (a) Nu vs K_2/K_1 ($n = 2$, $d_1 = d_2$, $\alpha_1 = \alpha_2$), (b) Nu vs d_1/H ($n = 2$, $K_2/K_1 = 5$, $\alpha_1 = \alpha_2$).

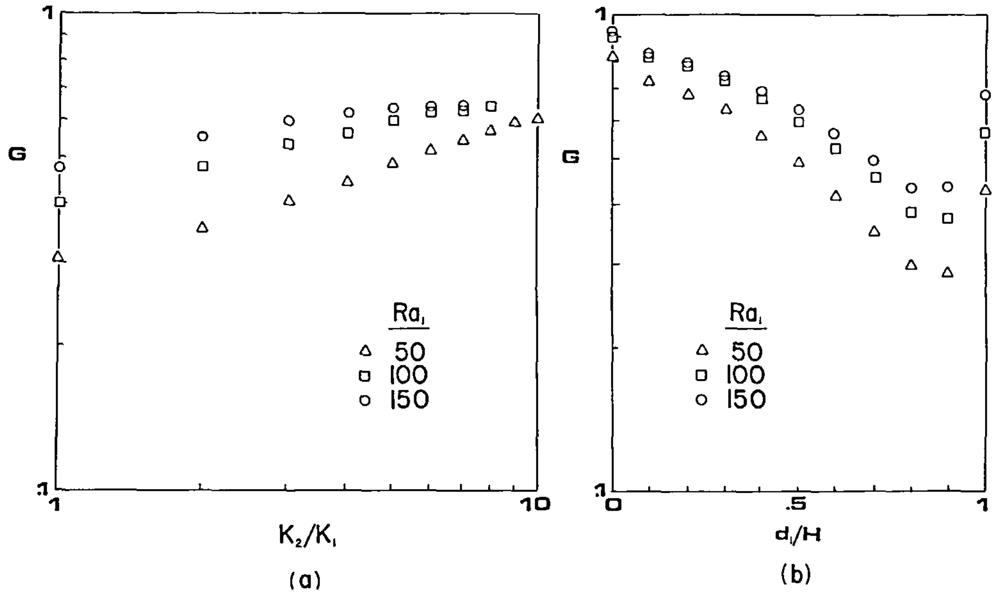

FIG. 8. Correlation of the heat transfer data of Figs. 10(a) and (b), (a) G vs K_2/K_1, (b) G vs d_1/H.

sublayers. Since each sublayer is homogeneous, the order of magnitude of the vertical boundary layer thickness in each sublayer is [8] [see also equation (20)]

$$\delta_i \sim d_i\left(\frac{g\beta K_i d_i \Delta T/2}{\alpha\nu}\right)^{-1/2}, \quad i = 1, 2. \tag{21}$$

Then, looking at the variable-thickness boundary layer coating one vertical wall, the total heat transfer rate through the wall is of order

$$Q = Q_1 + Q_2 \sim kd_1\frac{\Delta T/2}{\delta_1} + kd_2\frac{\Delta T/2}{\delta_2}, \tag{22}$$

where, for example, Q_1 is the heat transfer collected over the sublayer vertical boundary layer of thickness δ_1 and height d_1. Recalling the dimensionless notation used throughout this study

$$Nu = \frac{Q}{kH\Delta T/L}, \quad Ra_1 = \frac{g\beta HK_1\Delta T}{\alpha\nu}, \tag{23}$$

the scaling law (22) reduces to

$$Nu \sim 2^{-3/2}\frac{L}{H}Ra_1^{1/2}\left[\left(\frac{d_1}{H}\right)^{1/2} + \left(\frac{K_2}{K_1}\right)^{1/2}\left(1-\frac{d_1}{H}\right)^{1/2}\right]. \tag{24}$$

Based on the same argument, if the system contains n horizontal sublayers, the scaling law (24) assumes the more general form

$$Nu \sim 2^{-3/2}\frac{L}{H}Ra_1^{1/2}\sum_{i=1}^{n}\left(\frac{K_i d_i}{K_1 H}\right)^{1/2}. \tag{25}$$

To test the validity of the above scaling, the heat transfer results of Figs. 7(a) and (b) have been replotted in Figs. 8(a) and (b) as the new group

$$G = \frac{Nu}{2^{-3/2}(L/H)\,Ra_1^{1/2}\sum_{i=1}^{n}(K_i d_i/K_1 H)^{1/2}} \sim O(1). \tag{26}$$

It is clear that in the high Ra cases covered by the heat transfer calculations reported in Figs. 8(a) and (b), the G group is of $O(1)$, in agreement with the predictions based on scale analysis. Therefore, the Nusselt number expression (25) provides an adequate means for predicting the scale of heat transfer in a multilayered horizontal porous medium in the boundary layer regime.

4. CONCLUSIONS

The object of this study has been to document the effect of porous medium inhomogeneity on the natural convection heat transfer through systems heated in the horizontal direction. Special emphasis was placed on the effect of nonuniform permeability. Section 2 was devoted to porous systems composed of sublayers oriented vertically. Numerical solutions to the convection problem showed that:

(a) discontinuities in porous medium permeability cause cusps in both streamline and isotherm patterns;
(b) the flow prefers to inhabit the sublayer(s) of highest permeability;
(c) the heat transfer rate is influenced substantially by the thickness and permeability of the peripheral sublayers adjacent to the heated vertical walls [Figs. 4(a) and (b)];
(d) an important dimensionless parameter is the ratio of sublayer thickness divided by the boundary layer thickness based on sublayer

properties [Figs. 5(a) and (b)]: this parameter was used to correlate the heat transfer data.

Section 3 focused on convection in porous systems with horizontal sublayers. The new feature revealed by the patterns of Figs. 6(a) and (b) is the presence of vertical boundary layers of nonuniform thickness: this feature is due to the fact that the constant-permeability sublayers are normal to the differentially heated side walls. Numerical heat transfer calculations showed that the total heat transfer rate through horizontally layered systems depends strongly on the relative permeability and thickness of the sublayers [Figs. 7(a) and (b)]. The heat transfer data were correlated via scaling arguments (Fig. 8).

Acknowledgement—This research was supported in part by National Science Foundation Grant No. MEA-82-07779.

REFERENCES

1. P. Cheng, Heat transfer in geothermal system. *Adv. Heat Transfer* **14**, 1–105 (1979).
2. K. J. Schneider, Investigation of the influence of free thermal convection on heat transfer through granular material, *International Institute of Refrigeration, Proceedings*, p. 247 (1963).
3. G. Mordchelles-Regnier, P. Micheau, A. Pirovano, C. Jumentier, J. S. Terpstra, Y. Lecourt, P. Cave and M. Breuille, Recherches Recentes Effectuees en France sur L'Isolation Thermique des Reacteures Nucleaires, International Atomic Energy Agency, p. 529. Vienna (1969).
4. S. Klarsfeld, Champs de Temperature Associes aux Mouvements de Convection Naturelle dans un Milieu Poreux Limite, *Revue Gén. Thermique* **108**, 1403–1423 (1970).
5. C. G. Bankvall, Natural convection in vertical permeable space, *Warme- und Stoffübertragung* **7**, 22–30 (1974).
6. B. K. C. Chan, C. M. Ivey and J. M. Barry, Natural convection in enclosed porous media with rectangular boundaries, *J. Heat Transfer* **92**, 21–27 (1970).
7. P. J. Burns, L. C. Chow and C. L. Tien, Convection in a vertical slot filled with porous insulation, *Int. J. Heat Mass Transfer* **20**, 919–926 (1977).
8. J. W. Weber, The boundary layer regime for convection in a vertical porous layer, *Int. J. Heat Mass Transfer* **18**, 569–573 (1975).
9. A. Bejan, On the boundary layer regime in a vertical enclosure filled with a porous medium, *Lett. Heat Mass Transfer* **6**, 93–102 (1979).
10. P. G. Simpkins and P. A. Blythe, Convection in a porous layer, *Int. J. Heat Mass Transfer* **23**, 881–887 (1980).
11. P. A. Blythe and P. G. Simpkins, Thermal convection in a rectangular cavity, in *Physiochemical Hydrodynamics*, Vol. 2, p. 511. Advance, New York (1977).
12. K. L. Walker and G. M. Homsy, Convection in a porous cavity, *J. Fluid Mech.* **87**, 449–474 (1978).
13. A. Bejan and C. L. Tien, Natural convection in a horizontal porous medium subjected to an end-to-end temperature difference, *J. Heat Transfer* **100**, 191–198 (1978).
14. C. E. Hickox and D. K. Gartling, A numerical study of natural convection in a horizontal porous layer subjected to an end-to-end temperature difference, *J. Heat Transfer* **103**, 797 (1981).
15. K. T. Yang and J. R. Lloyd, *Natural Convection Workshop Proceedings*, Breckenridge, Colorado, 19–21 July (1982). Sponsored by the National Science Foundation and the University of Notre Dame.
16. R. McKibbin and P. A. Tyvand, Anisotropic modeling of thermal convection in multilayered porous media, *J. Fluid Mech.* **118**, 315–339 (1982).
17. D. N. de G. Allen and R. V. Southwell, Relaxation methods applied to determine the motion, in two dimensions, of a viscous fluid past a fixed cylinder, *Q. J. Mech. Appl. Math.* **8**, 129–145 (1955).
18. L. C. Chow and C. L. Tien, An examination of four differencing schemes for some elliptic-type convection equations, *Num. Heat Transfer* **1**, 87 (1978).
19. C. Y. Chow, *An Introduction to Computational Fluid Mechanics*. New York (1979).

CONVECTION NATURELLE DANS UN MILIEU POREUX A COUCHES VERTICALES OU HORIZONTALES ET CHAUFFE LATERALEMENT

Résumé—On étudie numériquement l'effet d'une perméabilité et d'une diffusivité thermique non uniformes pour un système poreux chauffé latéralement. La première partie de l'étude, section 2, s'intéresse aux systèmes composés de sous-couches verticales. On montre que le flux thermique de chaleur est sensiblement influencé par l'épaisseur et la perméabilité des couches périphériques adjacentes aux parois verticales chauffées. Les résultats de transfert thermique sont unifiés en utilisant le rapport de l'épaisseur de la sous-couche périphérique à l'épaisseur de la couche limite basée sur les propriétés de la sous-couche périphérique. La second partie de l'étude, en section 3, concerne des systèmes poreux composés de sous-couches horizontales avec des perméabilités différentes. On montre qu'à cause de l'absence d'homogénéité, les parois verticales du système sont bordées par des couches limites dont les épaisseurs varient d'une sous-couche à l'autre. Une loi générale d'échelle est donnée pour les systèmes à couches horizontales.

FREIE KONVEKTION IN VERTIKAL UND HORIZONTAL GESCHICHTETEN, SEITLICH BEHEIZTEN, PORÖSEN MEDIEN

Zusammenfassung—Es wird der Einfluß der ungleichförmigen Permeabilität und Wärmeleitfähigkeit auf die freie Konvektion in einem porösen, seitlich beheizten System numerisch untersucht. Der erste Teil der Abhandlung konzentriert sich in Abschnitt 2 auf Systeme, die aus vertikalen Teilschichten bestehen. Es wird gezeigt, daß der Wärmeübergang wesentlich von der Dicke und der Permeabilität der an die beheizten vertikalen Wände angrenzenden Randschichten abhängt. Die Ergebnisse des Wärmeübergangs werden dargestellt, indem der Quotient aus der Dicke der Randschicht und der mit den Stoffwerten der Randschicht gebildeten Grenzschicht verwendet wird. Der zweite Teil der Untersuchung handelt in Abschnitt 3 von porösen Systemen, die aus horizontalen Teilschichten mit unterschiedlichen Permeabilitäten bestehen. Es wird gezeigt, daß sich wegen dieses Mangels an Homogenität an den vertikalen Wänden des Systems Grenzschichten befinden, deren Dicke von einer Teilschicht zur nächsten variiert. Es wird über ein allgemeines Ähnlichkeitsgesetz der Wärmeübertragung für horizontal geschichtete Systeme berichtet.

ЕСТЕСТВЕННАЯ КОНВЕКЦИЯ В НАГРЕВАЕМЫХ СБОКУ ВЕРТИКАЛЬНЫХ И ГОРИЗОНТАЛЬНЫХ СЛОЯХ ПОРИСТЫХ СРЕД

Аннотация—Численно исследуется влияние неоднородной проницаемости и температуропроводности на естественную конвекцию в нагреваемой сбоку пористой системе. Первая часть исследования (параграф 2) посвящена системам, состоящим из вертикальных подслоев. Показано, что на интенсивность теплопереноса существенное влияние оказывают толщина и проницаемость периферийных подслоев, прилегающих к нагретым вертикальным стенкам. Результаты по теплопереносу обрабатываются с помощью отношения толщины периферийного подслоя к толщине пограничного слоя, вычисляемой по характеристикам периферийного подслоя. Вторая часть исследования (параграф 3) посвящена пористым системам, состоящим из горизонтальных подслоев с различными проницаемостями. Показано, что из-за отсутствия однородности на вертикальных стенках системы образуются пограничные слои, толщина которых изменяется от подслоя к подслою. Предложен общий закон подобия теплопереноса для систем с горизонтальными слоями.